Torsemide and Furosemide as Green Inhibitors for the Corrosion of Mild Steel in Hydrochloric Acid Medium

DATASET · MAY 2013

2 AUTHORS, INCLUDING:

Hari Kumar S.
VIT University
3 PUBLICATIONS **20** CITATIONS

SEE PROFILE

I&EC research
Industrial & Engineering Chemistry Research

Article

pubs.acs.org/IECR

Torsemide and Furosemide as Green Inhibitors for the Corrosion of Mild Steel in Hydrochloric Acid Medium

Sappani Hari Kumar[†] and Sambantham Karthikeyan*[,‡]

[†]Materials Chemistry Division, School of Advanced Sciences, VIT University, Vellore 632014, Tamilnadu, India

[‡]Centre for Nanobiotechnology, VIT University, Vellore 632014, Tamilnadu, India

Supporting Information

ABSTRACT: The performance of torsemide and furosemide drugs as corrosion inhibitors for mild steel in 1 N HCl was thoroughly investigated by weight loss and electrochemical methods. The inhibition efficiencies of drugs obtained by all methods were in good agreement with each other. Torsemide exhibited higher inhibition efficiencies than furosemide in all the experimental studies. Polarization studies revealed that the inhibiting action of the compounds is under mixed control. The free energy of adsorption and the influence of temperature on the adsorption of inhibitors onto a mild steel surface have been reported. The adsorption of the compounds was found to obey the Langmuir adsorption isotherm. The mechanism of inhibition and formation of the Fe−inhibitor complex were confirmed by FT-IR and UV−visible absorption spectral analysis. The scanning electron microscopy (SEM) and atomic force microscopy (AFM) results established the formation of a protective layer on the mild steel surface. Quantum chemical calculations were applied to correlate the inhibition performance of inhibitors with their electronic structural parameters.

1. INTRODUCTION

Acid solutions are commonly used in gas and oil exploration, for pickling, cleaning, and descaling, of steel structures, processes which normally result in dissolution of the metal. A common method followed to inhibit corrosion of metals and alloys deployed in an aggressive medium is the addition of some compounds to the medium which is in contact with surface in order to reduce the corrosion rate and reaction. A number of compounds have been reported as corrosion inhibitors for mild steel in acidic environments.[1−8] Those compounds typically contain nitrogen, oxygen, or sulfur in a conjugated system, and adsorption of the molecules occurs on the metal surface by forming a thin layer over the metal surface. The adsorption bond strength depends on the nature of the metal, inhibitor structure, concentration of electrolyte, as well as temperature.

The adsorption is due to the attractive forces generated between the metal and the adsorbate. On the basis of the type of forces, adsorption can be physisorption, chemisorption, or a combination of both. Physisorption is the electrostatic attractive force between inhibiting ions and the electrically charged surface of the metal. Chemisorption is an interaction between the metal and unshared electron pairs of the adsorbate to form a coordinate bond. It may take place in the presence of heteroatoms (S, N, and O), with a lone pair of electrons and aromatic rings in the adsorbed molecules.[9−12] According to this mechanism, a reduction of either the anodic or the cathodic reaction or both arises from the adsorption of inhibitor on the corresponding active sites.[13] Various mechanisms for inhibition must be considered due to the various changes created by changing factors, such as the medium and inhibitor in the system.[14,15]

Despite the wide range of available organic compounds, the final choice of the inhibitor for a particular application is restricted by several factors, including increased environmental awareness and the need to promote environmentally friendly processes, coupled with the specificity of action of most acid inhibitors, which often necessitates the combined action of compounds to achieve effective corrosion inhibition. Consequently, there exists a need to develop inexpensive and environmently friendly inhibitors. In recent years researchers have paid attention to the development of drugs as inhibitors for the corrosion of metals in acid media.[16−26]

The aim of the present work is to study the furosemide and torsemide drugs as alternative corrosion inhibitors for mild steel in 1 N HCl solution using chemical and electrochemical techniques. These drugs are diuretics used in the treatment of congestive heart failure and management of hypertension. No concrete report is seen for the employment of these compounds as corrosion inhibitors in 1 N HCl medium. Quantum chemical calculations have been performed using DFT, and various quantum chemical indices were calculated and correlated with the inhibitive effect of furosemide and torsemide. SEM, EDX, and AFM of the mild steel surface have been recorded to examine the changes in surface morphology of mild steel covered with a thin layer of furosemide and torsemide. UV−visible spectroscopic studies of the testing solutions before and after corrosion experiments were performed and discussed. The effect of temperature on different concentrations of inhibitors has been analyzed. Thermodynamic parameters of the corrosion reaction have been obtained for the above studies.

Received: March 13, 2013
Revised: April 13, 2013
Accepted: May 10, 2013

   dx.doi.org/10.1021/ie400815w | *Ind. Eng. Chem. Res.* XXXX, XXX, XXX−XXX

2. EXPERIMENTAL SECTION

2.1. Materials. Mild steel specimens of composition C = 0.08%, P = 0.07%, Si = 0%, S = 0%, Mn = 0.41%, and balance Fe with size 1 × 4 cm^2 were used for weight loss and electrochemical studies. The solutions of 1 N HCl were prepared by dilution of 37% analytical grade HCl with double-distilled water. Two drugs, viz., furosemide and torsemide, were procured from Aventis and Cipla Pharmaceuticals Limited. The structures of the antibiotics are given in Figure 1. Prior to the measurements, the mild steel samples were polished with different emery papers, rinsed with double-distilled water, degreased in acetone, and then dried at room temperature.

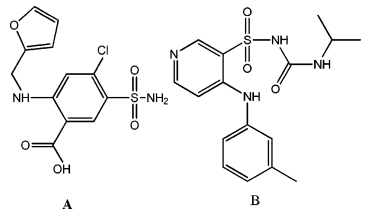

Figure 1. Structures of the inhibitors (A) furosemide and (B) torsemide.

2.2. Weight Loss Measurements. The weight loss method was used to optimize the concentration of the inhibitors. The weight loss method gave a baseline to the other well established corrosion control techniques, such as electrochemical impedance spectroscopy, Tafel polarization measurements, and linear polarization measurements. Weight loss measurements have been done according to the method described earlier.[27] Weight loss measurements were performed on the previously weighed mild steel specimens of size 4 cm × 1 cm × 0.2 cm in 100 mL of 1 N HCl solutions with and without the additions of various concentrations of the inhibitors at three different temperatures. The specimens were immersed for 3 h in the test solution. After the immersion the specimens were withdrawn, rinsed with distilled water, dried, and weighed accurately. The experiments were carried out in triplicate, and the average values are reported. The reproducibility of the experiment was greater than 95%. The inhibition efficiency (I.E.) and surface coverage (θ) were determined by using the following equations:

$$\text{I.E. } (\%) = \frac{w_0 - w_1}{w_0} \times 100 \quad (1)$$

$$\theta = \frac{w_0 - w_1}{w_0} \quad (2)$$

where w_0 and w_1 are the weight loss values in the absence and presence of inhibitors, respectively. θ is the degree of surface coverage of the inhibitors. The corrosion rate (CR) was calculated from the following equation:

$$\text{CR} = \frac{534w}{DAT} \text{ mpy} \quad (3)$$

where w is the weight loss of mild steel (mg), D is the density of mild steel, T is the time of immersion, and A is the area of the specimen exposed to the corrosive solution.

2.3. Electrochemical Measurements. A conventional three-electrode assembly was used to carry out the electrochemical experiments at ambient temperature. A mild steel specimen of 1 cm^2 dimension was used as working electrode, a platinum wire as a counter electrode, and a saturated calomel electrode (SCE) via luggin capillary probe as a reference electrode. The luggin capillary was kept in a manner that its tip is very close to the working electrode to minimize IR drop. All experiments were carried out in the presence and absence of different concentrations of the inhibitors used in weight loss measurements. All electrochemical measurements were carried out using a EG & G Princeton Applied Research Model (7310) Potentiostat. All the experiments were carried out after immersion of mild steel for 30 min in 1 N HCl with the above conditions. The working electrode was first immersed in the corrosive medium for 30 min to access a steady state open circuit potential (OCP). After this time the steady state OCP corresponding to the corrosion potential of the working electrode was obtained.

Potentiodynamic polarization curves were obtained by changing the electrode potential from the cathodic to anodic direction (OCP ± 250 mV) with a scan rate of 1 mV s^{-1}. The anodic and cathodic curves of linear Tafel plots were extrapolated to obtain the corrosion current (I_{corr}) and corrosion potential (E_{corr}). Impedance measurements were carried out in the frequency range 100 kHz to 0.01 Hz under potentiostatic conditions, with an amplitude of 10 mV peak to peak using an ac signal at E_{corr}.

2.4. Scanning Electron Microscopy. Mild steel specimens of size 4 cm × 1 cm × 0.25 cm were immersed in 1 N HCl in the absence and presence of 14 × 10^{-4} M furosemide and torsemide for 3 h. Then the specimens were removed and washed with distilled water and dried at ambient temperature. The chemical composition of the corrosion products was recorded with an EDX detector coupled with the SEM.

2.5. Atomic Force Microscopy. The morphology of the mild steel surface was investigated by atomic force microscopy. For AFM analysis the mild steel specimens of size 1 cm × 1 cm × 0.25 cm were immersed in the test solution in the absence and presence of inhibitors for 3 h at room temperature. Then the specimens were cleaned with distilled water, dried, and used for AFM. The AFM analyses were carried out using a Nanosurf Easyscan2 instrument.

2.6. UV−Visible Spectroscopy. UV−visible absorption spectroscopy was carried out for the 1 N HCl solution containing 14 × 10^{-4} M furosemide and torsemide before and after a 3 h immersion of mild steel at room temperature using a Jasco UV-NIR spectrometer.

2.7. FT-IR Spectroscopy. FT-IR spectra were recorded with the frequency ranging from 4000 to 400 cm^{-1} for both the furosemide and torsemide powders as well as the powders adsorbed on the mild steel in 1 N HCl solution in a KBr matrix using a Shimadzu IR Affinity-1 model instrument.

2.8. Theoretical Study. Quantum calculations were performed with the Gaussian 03 software package. The molecular structures of the neutral species were geometrically optimized using the density functional theory (DFT)/B3LYP method (Becke's three-parameter hybrid Hartree−Fock (HF)/DFT exchange functional (LYP)) with the basis set 6-31G(d,p). Quantum chemical parameters such as the energy of the highest occupied molecular orbital (HOMO), the lowest unoccupied molecular orbital (LUMO), the energy gap between E_{LUMO} and E_{HOMO} ($\Delta E = E_{LUMO} - E_{HOMO}$), dipole moment ($\mu$), total negative charges on atoms (TNC), electronegativity (χ), chemical hardness (η), absolute softness (σ), total energy (TE), and fraction of electrons transferred

dx.doi.org/10.1021/ie400815w | Ind. Eng. Chem. Res. XXXX, XXX, XXX−XXX

from the inhibitors to the iron surface (ΔN) were calculated using this method.

3. RESULTS AND DISCUSSION

3.1. Weight Loss Measurements. The effect of the addition of furosemide and torsemide at various concentrations on mild steel corrosion at 303 K after a 3 h immersion was investigated by a weight loss method. Corrosion parameters such as inhibition efficiency (I.E.), corrosion rate (CR), and surface coverage (θ) at various concentrations of inhibitors are presented in Table 1. It is observed from Table 1 that at 303 K the inhibition efficiency increased and the corrosion rate decreased on increasing the concentrations of furosemide and torsemide. This behavior is attributed to the increase in adsorption of inhibitors to the mild steel/acid interface to increase the concentration of inhibitors. Furosemide and torsemide showed a maximum inhibition efficiency of 84.73 and 88.75 at an optimum concentration of 14×10^{-4} M at 303 K, respectively. A further increase in concentration of the inhibitors did not bring any significant changes in inhibition efficiency and corrosion rates.

Table 1. Corrosion Parameters for Mild Steel in 1 N HCl in the Presence of Different Concentrations of Furosemide and Torsemide Obtained from Weight Loss Measurements at 303 K

inhibitor conc (M)	weight loss (g)	inhibition efficiency (%)	corrosion rate (mg cm^{-2} h^{-1})	surface coverage (θ)
blank	0.0249		2.07	
		Furosemide		
2×10^{-4}	0.0087	65.06	0.72	0.6506
6×10^{-4}	0.0072	71.08	0.60	0.7108
10×10^{-4}	0.0060	75.90	0.50	0.8590
14×10^{-4}	0.0038	84.73	0.31	0.8473
		Torsemide		
2×10^{-4}	0.0054	78.31	0.45	0.7831
6×10^{-4}	0.0043	82.73	0.35	0.8273
10×10^{-4}	0.0034	86.34	0.28	0.8634
14×10^{-4}	0.0028	88.75	0.23	0.8875

To study the effects of temperature on corrosion inhibition properties, the mild steel specimens were exposed to acid solutions containing different concentrations of inhibitors at four different temperatures, that is, 303, 313, 323, and 333 K. The effect of inhibitor concentration on the inhibition efficiency of mild steel in 1 N HCl at different temperatures is shown in Figure 2. The calculated inhibition efficiencies at different temperatures are listed in the Supporting Information (Table S1) for furosemide and torsemide. It is evident from Figure 2 and Table S1 that the inhibition efficiency increased with an increase in concentration of inhibitors at different temperatures and that it decreased with an increase in temperature. This is due to the fact that at higher temperatures the metal dissolution process is enhanced and the adsorbed inhibitor molecules are partially desorbed from the metal surface.[28]

3.2. Potentiodynamic Polarization Measurements. This method involves the monitoring of the current that is produced as a function of time or potential by varying the potential of the working electrode. Tafel polarization curves for mild steel in 1 N HCl at different concentrations of furosemide and torsemide are shown in Figure 3. It can be observed that the presence of furosemide and torsemide caused a prominent decrease in corrosion rate. This is supported by the shift of anodic curves to more positive potentials and the shift of cathodic curves to more negative potentials, and by the lower values of corrosion current densities equally. It is noted that cathodic Tafel curves are more linear than anodic Tafel curves over the applied potential range. This is attributed to the deposition of corrosion products on the mild steel surface.[29]

The polarization parameters E_{corr}, I_{corr}, and anodic and cathodic Tafel slopes (β_a, β_c) are listed in Table 2. Inhibition efficiency (I.E.) values were calculated from the equation

$$\text{I.E.}(\%) = \frac{I_{corr} - I_{corr(i)}}{I_{corr}} \times 100 \quad (4)$$

where $I_{corr(i)}$ is the corrosion current density in the presence of the inhibitor and I_{corr} is the corrosion current density in the absence of inhibitor in the solution. It is clear that the hydrogen evolution reaction (cathodic reaction) and dissolution of metal (anodic reaction) have been retarded. There is no significant change in the E_{corr} values in the presence and absence of inhibitors.

The corrosion of mild steel in acid solutions is controlled by the hydrogen evolution reaction, that is, the cathodic reaction.[30]

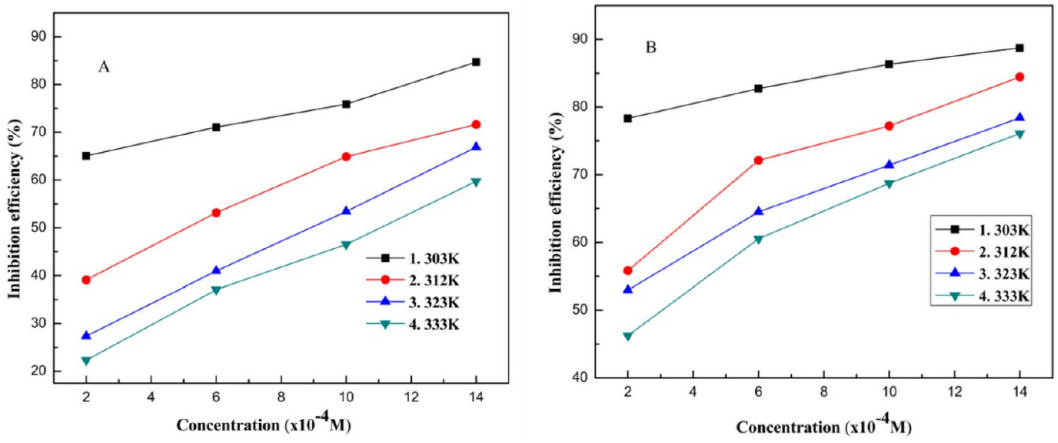

Figure 2. Variation of inhibition efficiency in 1 N HCl in the presence of different concentrations of (A) furosemide and (B) torsemide at different temperatures.

dx.doi.org/10.1021/ie400815w | Ind. Eng. Chem. Res. XXXX, XXX, XXX−XXX

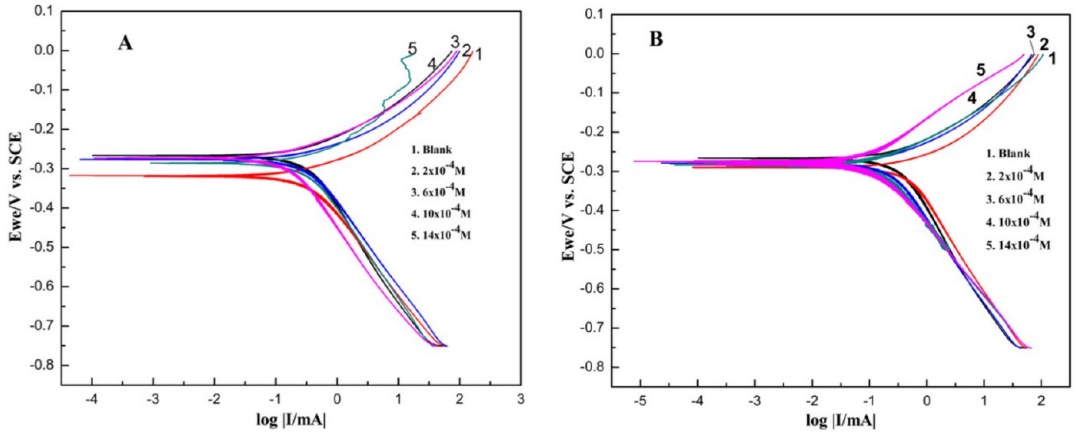

Figure 3. Tafel polarization curves for mild steel immersed in various concentrations of (A) furosemide and (B) torsemide in 1 N HCl.

Table 2. Polarization Parameters for Mild Steel in 1 N HCl Containing Different Concentrations of Inhibitors

inhibitor conc (M)	E_{corr} (mV vs SCE)	I_{corr} (μA cm^{-2})	β_a (mV dec^{-1})	β_c (mV dec^{-1})	inhibition efficiency (%)	surface coverage (θ)
blank	−349	873.11	112.3	257.9		
			Furosemide			
2×10^{-4}	−327.11	345.09	121.4	228.9	60.47	0.6047
6×10^{-4}	−317.33	222.81	117.7	223.4	66.89	0.6689
10×10^{-4}	−298.21	199.71	112.3	216.7	77.12	0.7712
14×10^{-4}	−285.49	122.81	101.2	206.7	85.93	0.8593
			Torsemide			
2×10^{-4}	−328.58	305.8	137.9	246.1	64.97	0.6497
6×10^{-4}	−308.22	215.56	114.8	223.5	75.31	0.7531
10×10^{-4}	−291.70	187.98	98.7	191.0	78.47	0.7847
14×10^{-4}	−260.45	106.02	92.4	175.7	87.85	0.8785

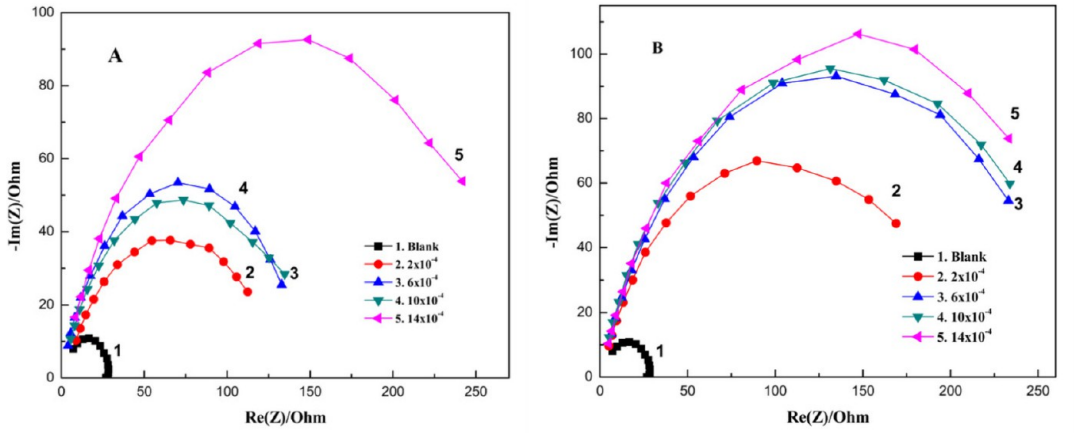

Figure 4. Nyquist curves for mild steel immersed in various concentrations of (A) furosemide and (B) torsemide in 1 N HCl.

The adsorbed furosemide and torsemide molecules retard the electrochemical reaction on the surface of the mild steel due to the covered surface sites. The furosemide and torsemide affect the rate of corrosion through the variation of surface coverage, which results in reducing the H^+ concentration and the corresponding hydrogen evolution over potential.[31] The change in the cathodic Tafel slopes (β_c) of the inhibited system indicate the influence of inhibitor molecules on the kinetics of hydrogen evolution.[32] This decrease in gas evolution is due to the increase in the energy barrier for proton discharge.[33] The anodic curves of the electrode in HCl containing furosemide and torsemide shifted to the direction of current reduction, which suggested that the inhibitors also suppress the anodic reaction. It is reported in the literature[34] that (i) if the displacement in E_{corr} is >85 mV with repect to E_{corr}, the inhibitor can act as a cathodic or anodic type and (ii) if the displacement in E_{corr} is <85 mV, the inhibitor can be considered as a mixed type. In the present study the shift in E_{corr} values is in the range 21−79 mV for both the inhibitors, indicating that the furomide and torsemide have acted as a mixed inhibitor,[35] which is further evidenced from equal shifting of Tafel slopes.

From polarization results it is noted that the I_{corr} values decrease in the presence of various concentrations of furosemide and torsemide as compared with blank. It has been noticed that the corrosion current of torsemide decreases in greater values than furosemide. This reflects the enhanced

dx.doi.org/10.1021/ie400815w | Ind. Eng. Chem. Res. XXXX, XXX, XXX−XXX

power of torsemide molecules to inhibit mild steel corrosion in 1 N HCl solution, as compared with furosemide.

3.3. Electrochemical Impedance Spectroscopy. The kinetics of the electrode process and the surface properties has been investigated by impedance spectroscopy. Mechanistic information of the reaction at the surface can be explained from the shape of the Nyquist plots. This method is most widely used to study the corrosion inhibition process. Nyquist plots of mild steel in the absence and presence of furosemide and torsemide are presented in Figure 4. The charge transfer resistance (R_{ct}) and double-layer capacitance (C_{dl}) were the parameters obtained from the impedance spectroscopy. The inhibition efficiency is calculated from the R_{ct} values using the following formulas:

$$\text{I.E.}(\%) = \frac{R_{ct(i)} - R_{ct(b)}}{R_{ct(i)}} \times 100 \quad (5)$$

where $R_{ct(i)}$ and $R_{ct(b)}$ are the charge transfer resistances in the presence and absence of the inhibitors, respectively. The calculated electrochemical impedance parameters are given in Table 3. The equivalent circuit used for the study is Randle's

Table 3. Impedance Parameters for Mild Steel in 1 N HCl in the Absence and Presence of Different Concentrations of Inhibitors

inhibitor conc (M)	R_{ct} (Ω cm^2)	C_{dl} (μF cm^{-2})	τ (s)	IE (%)	surface coverage (θ)
blank	23.79	164.0	0.00045		
		Furosemide			
2×10^{-4}	131.7	157.1	0.00234	81.93	0.8193
6×10^{-4}	146.2	141.6	0.00239	83.7	0.8370
10×10^{-4}	253.7	134.7	0.00396	84.52	0.8452
14×10^{-4}	276.9	113.9	0.00365	91.40	0.9140
		Torsemide			
2×10^{-4}	180.3	152.4	0.00318	86.80	0.8680
6×10^{-4}	205.7	116.9	0.00278	88.43	0.8843
10×10^{-4}	244.5	114.0	0.00322	90.26	0.9026
14×10^{-4}	286.2	113.0	0.00374	91.68	0.9168

circuit, shown in Figure 5. In this circuit, R_{ct} is the charge transfer resistance, C_{dl} is the double-layer capacitance, and R_s is the solution resistance.

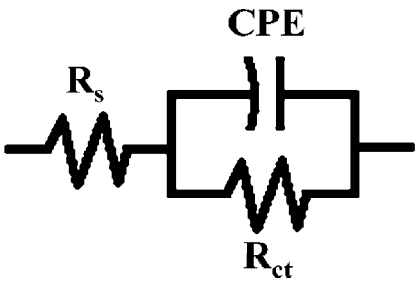

Figure 5. Electrical equivalent circuit.

From Figure 4 it was observed that high-frequency (HF) depressed charge-transfer semicircles were followed by an inductive loop in the low-frequency regions. The time constant of charge transfer resistance and double-layer capacitance was obtained from the HF semicircle.[36] The inductive loop at low frequency is due to the relaxation process obtained by adsorption species as Cl^-_{ads} and H^+_{ads} on the surface of the electrode.[37] The low-frequency inductive loop may also be attributed to nondissolution of the passivated surface at low frequencies. The relaxation time (τ) of the surface, that is, the time required for attaining the charge distribution to equilibrium is given by the following:

$$\tau = C_{dl}R_{ct} \quad (6)$$

The adsorption of inhibitor needs some time to attain equilibrium. This time is very short, as shown in Table 3. The time required to attain equilibrium increased with increase in the concentration of furosemide and torsemide. This is due to the increase in adsorption of inhibitor molecules on the mild steel surface.

It was observed from Table 3 that the R_{ct} values increased and C_{dl} values decreased with increase in concentrations of both furosemide and torsemide. This may be due to the increase in the surface coverage on the mild steel by the inhibitors, which led to the increase in inhibition efficiency. The C_{dl} is related to the thickness of the protective layer (d) by the following equation:[38]

$$C_{dl} = \frac{\varepsilon_0 A}{d} \quad (7)$$

where ε is the dielectric constant of the medium, ε_0 is the permittivity of the free space, and A is the effective surface area of the electrode. The decrease in C_{dl} leads an increase in thickness of the double layer, which confirms that the furosemide and torsemide molecules inhibit the corrosion by adsorption at the mild steel/solution interface. The changes in C_{dl} values are due to the replacement of water molecules by furosemide and torsemide.

The results of weight loss and polarization studies have agreed very well. A minor deviation in inhibition efficiencies noted from impedance measurements might be due to development of heterogeneities in the surface by the attack of chloride ions along with polarizability of metal surfaces.

3.4. Activation Parameters. Weight loss measurements were carried out in the temperature range of 303−333 K in the presence and absence of different concentrations of furosemide and torsemide to calculate the activation parameters of the above corrosion process. Arrhenius and transition state equations were used to study the influence of temperature on rate of corrosion.[39]

$$\log(CR) = \frac{-E_a}{2.303RT} + \log \lambda \quad (8)$$

$$\text{CR} = \frac{RT}{Nh} \exp\left(\frac{\Delta S^*}{R}\right) \exp\left(-\frac{\Delta H^\circ_a}{RT}\right) \quad (9)$$

where E_a is apparent activation energy, λ the preexponential factor, ΔH^* the apparent enthalpy of activation, ΔS^* the apparent entropy of activation, h Planck's constant, and N the Avogadro number, respectively.

The activation energy and the pre-exponential factors at different concentrations of the inhibitors were calculated from linear regression between log CR and $1/T$ as shown the Figure S1 (Supporting Information). The calculated values are presented in Table 4. It is inferred from the table that the apparent activation energy of furosemide increased with increase of its concentration. This increase in apparent activation energy may be interpreted as physical adsorption.[40] The increased activation energy values could decrease the

dx.doi.org/10.1021/ie400815w | Ind. Eng. Chem. Res. XXXX, XXX, XXX−XXX

Table 4. Thermodynamic Activation Parameters for Mild Steel in 1 N HCl in the Absence and Presence of Different Concentrations of Furosemide and Torsemide

inhibitor	conc (10^{-4} M)	E_a (kJ mol^{-1})	λ (mg cm^{-2})	ΔH^* (kJ mol^{-1})	ΔS^* (J mol^{-1} K^{-1})
	blank	73	9.79×10^{12}	70	−5
furosemide	2	94	2.29×10^{16}	92	59
	6	95	1.72×10^{16}	92	57
	10	96	1.92×10^{16}	93	58
	14	99	5.43×10^{16}	97	67
torsemide	2	97	3.31×10^{16}	95	62
	6	96	1.75×10^{16}	94	57
	10	96	1.36×10^{16}	93	55
	14	94	6.42×10^{15}	92	49

adsorption of inhibitor on the mild steel surface with increase in both temperature and corrosion rates, since the greater area of metal has been exposed to the acid environment.[41] This is confirmed by the increase in λ values, which is related to the number of active centers on the metal surface.[42]

The increase in apparent activation energy after the addition of torsemide to a 1 N HCl solution indicated its physical adsorption (electrostatic) in the first stage. When a higher concentration of torsemide is used, the activation energy gradually decreased. This can be due to the chemisorption process. Similar behavior is reported by Ashassi-Sorkhabi et al.[43] In torsemide, on increasing the inhibitor concentrations, the number of active centers decreases, which is evidenced by the lower λ values.

According to eq 8 the corrosion rate (CR) is being affected by both E_a and λ. Generally the influence of E_a on mild steel corrosion is higher than that of λ. In the present study E_a and λ increased with concentration for furosemide and decreased with an increase in concentration for torsemide (the higher E_a and lower λ led to lower corrosion rate). Hence it is clear that higher values of E_a were the dominant factor affecting the corrosion rate of mild steel in 1 N HCl in the presence of furosemide. For torsemide, at lower concentration, the enhancement in activation energy is the determining factor to lower corrosion rate.

Figure S2 in the Supporting Information shows a plot of $\log(CR/T)$ vs $1/T$. Straight lines were obtained with a slope equal to $(-\Delta H^*/(2.303R))$ and the intercept equal to $[\log(R/Nh) + (\Delta S^*/(2.303R))]$, from which the values of ΔH^* and ΔS^* were calculated and listed in Table 4. Inspection of these data reveals that the thermodynamic parameters (ΔH^* and ΔS^*) of the dissolution reaction of mild steel in 1 N HCl in the presence of furosemide and torsemide are higher than those in their absence. The positive sign of the enthalpies reflects the endothermic nature of the mild steel dissolution process, indicating that dissolution of mild steel is difficult.[44]

On comparing the values of entropy of activation (ΔS^*) given in Table 4, it is clear that the entropy of activation increased positively in the presence of furosemide. The increase of ΔS^* could be due to an increase in disorderliness of molecules.[45] Hence, higher values of ΔS^* for torsemide confirm the disorderliness of molecules.

3.5. Adsorption Isotherm. The interaction of inhibitor molecules with the mild steel surface can be understood from the adsorption isotherms. The adsorption on the corroding surfaces does not reach the equilibrium; instead they tend to attain a steady state adsorption. The adsorption steady state has a tendency to become a quasi-equilibrium state when the corrosion rate is very low. In this situation, it is reasonable to consider the quasi-equilibrium adsorption in a thermodynamic way using the appropriate equilibrium isotherms.[46] The efficiencies of furosemide and torsemide mainly depend on their ability to adsorb on the mild steel surface. The degree of surface coverage (θ) for various concentrations of inhibitors in 1 N HCl has been calculated from weight loss, polarization, and electrochemical impedance studies and was tested diagrammatically for fitting the appropriate adsorption isotherm. The plot C_{inh}/θ versus C_{inh} (Figure 6A and B) gave a straight line with a slope of nearly unity, which suggests that the adsorption of furosemide and torsemide obeyed the Langmuir adsorption isotherm. The Langmuir adsorption isotherm is given by the following equation:

$$\frac{C_{inh}}{\theta} = \frac{1}{K_{ads}} + C_{inh} \tag{10}$$

where C_{inh} is the concentration of the inhibitor and K_{ads} is the adsorption equilibrium constant for the adsorption desorption process.

The adsorption constant (K_{ads}) and free energy of adsorption (ΔG°_{ads}) were calculated using the following equation:

$$K_{ads} = \frac{1}{C_{inh}} \times \frac{\theta}{1-\theta} \tag{11}$$

$$\Delta G^\circ_{ads} = -2.303RT \log[55.5K_{ads}] \tag{12}$$

where 55.5 is the molar concentration of water in solution.[47] R is the universal gas constant, and T is the temperature. The values of adsorption constant (K_{ads}) and free energy of adsorption (ΔG°_{ads}) at different temperatures are calculated and given in the Supporting Information (Table S2). The negative values of ΔG°_{ads} indicate the spontaneity of the adsorption process and the stability of the inhibitor film formed on the mild steel surface.[48] Generally it is accepted that the energy values of ΔG°_{ads} around −20 kJ mol^{-1} or lower indicate the electrostatic interaction between the charged metal surface and the charged inhibitor molecules, that is, physisorption, while those around −40 kJ mol^{-1} or higher involve charge sharing or charge transfer between the metal surface and the inhibitor molecules, that is, chemisorption.[49] The values of free energy of adsorption (ΔG°_{ads}) in our experiment lie within the range −28 to −34 kJ mol^{-1}, demonstrating that the adsorption is not a straightforward physisorption; however, it should involve some other interactions.[50] The high values of ΔG°_{ads} and K_{ads} indicate the high adsorption and higher inhibiting effect of torsemide than that of furosemide.

Thermodynamic parameters are considered very important in carrying out the studies about the adsorption of inhibitors on the metal surface. The heat of adsorption (ΔH°_{ads}) and entropy

dx.doi.org/10.1021/ie400815w | Ind. Eng. Chem. Res. XXXX, XXX, XXX−XXX

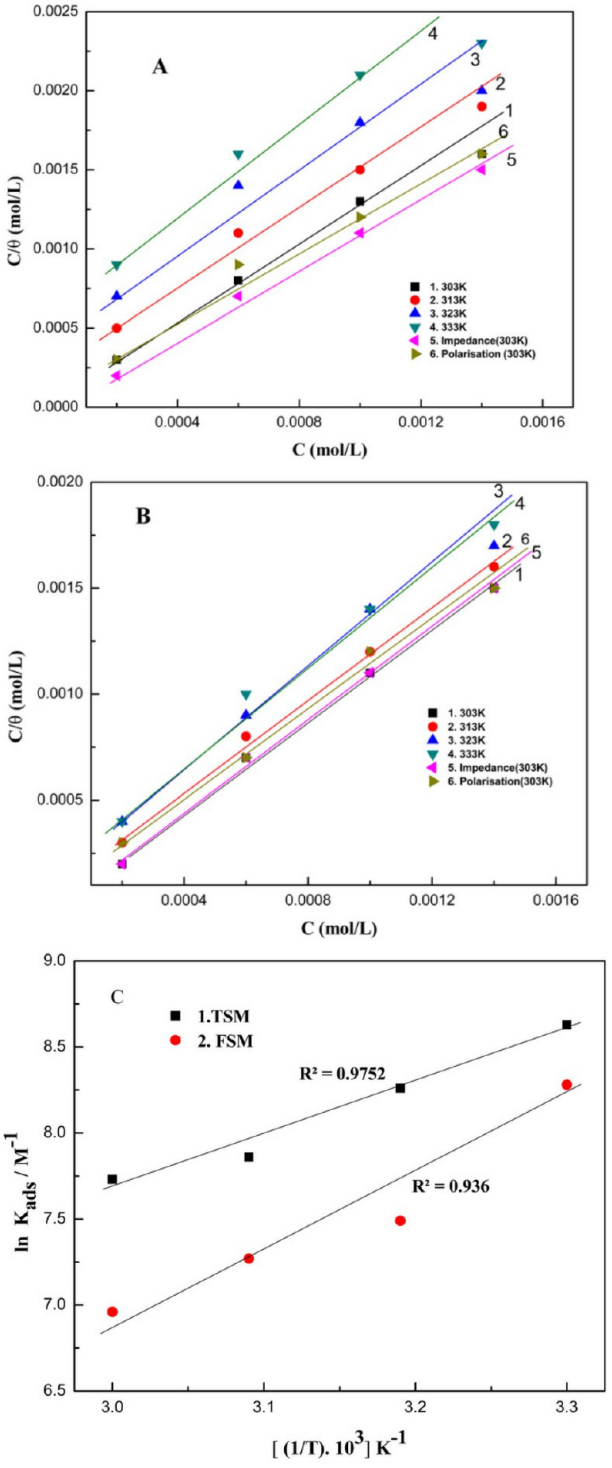

Figure 6. Langmuir's adsorption isotherm plots for (A) furosemide and (B) torsemide, and (C) plot of ln K_{ads} vs $1/T$.

of adsorption (ΔS°_{ads}) were calculated using the Van't Hoff equation.[51] According to the Van't Hoff equation,

$$\ln K_{ads} = \frac{-\Delta H^{\circ}_{ads}}{RT} + \text{constant} \quad (13)$$

To calculate heat of adsorption (ΔH°_{ads}) and entropy of adsorption (ΔS°_{ads}), ln K_{ads} was plotted against $1/T$ as shown in Figure 6C. The figure shows a straight line with slope equal to ($-\Delta H^{\circ}_{ads}/R$) and the intercept equal to ($\Delta S^{\circ}_{ads}/R$ + ln(1/55.5)). The calculated values of heat of adsorption (ΔH°_{ads}) and entropy of adsorption (ΔS°_{ads}) are listed in the Supporting Information (Table S3). The heat of adsorption (ΔH°_{ads}) can be considered as the standard adsorption heat (ΔH°_{ads}) under the experimental conditions.[52,53] The negative values of heat of adsorption (ΔH°_{ads}) indicate that the adsorption of both inhibitors is an exothermic process. It is reported that an exothermic adsorption process resembles either physisorption or chemisorption, while the endothermic adsorption process is applicable to chemisorptions.[54] The negative values of (ΔH°_{ads}) also suggest that inhibition efficiency (I.E.) decreased with an increase in temperature. This is due to desorption of adsorbed inhibitor molecules from the mild steel surface at higher temperatures. The value of entropy of adsorption (ΔS°_{ads}) is negative for furosemide adsorption and positive for torsemide adsorption. Since adsorption is an exothermic process, it is always supported by the decrease in entropy, which can be clearly depicted for furosemide from the calculated values. The positive value of (ΔS°_{ads}) for torsemide is a driving force for its adsorption on the mild steel surface. The increase in entropy can also be attributed to the increase in solvent entropy.

3.6. Scanning Electron Microscopy. SEM micrographs obtained from the mild steel surface before and after immersion in 1 N HCl solutions in the absence and presence of an optimum concentration (14×10^{-4}) of furosemide and torsemide are shown in Figure 7. A comparison can be done with the morphology of the micrographs. The morphology of mild steel immersed in unhibited solution in Figure 7A shows a very rough surface with cracks and pits due to the corrosion; from this it is concluded that the mild steel surface was greately damaged in the absence of inhibitors. Parts B and C of Figure 7 show the morphologies of mild steel immersed in 1 N HCl in the presence of furosemide and torsemide, respectively. The results proved that there is less damage on the mild steel surface in the presence of the inhibitors and that they protected the surface effectively in 1 N HCl. The morphology of mild steel immersed in torsemide is relatively smooth and less corroded when compared to the case of furosemide, which may be due to the strong interaction or adsorption of torsemide on the mild steel surface to reduce the corrosion.

3.6.1. EDX Analysis. The aim of this section is to confirm the results obtained from the gravimetric and electrochemical measurements, that a protective layer of furosemide and Torsemide is formed on the mild steel surface. EDX examinations of mild steel surfaces were performed in 1 N HCl in the absence and presence of furosemide and torsemide. EDX spectra were used to determine the elements present on the mild steel surface before and after immersion in the inhibitor solution. The percentage atomic content of Fe for mild steel immersed in 1 N HCl is 63%, and those for mild steel dipped in an optimum concentration of furosemide and torsemide are 65% and 66%, respectively. From Figure 8 the spectra of inhibited samples show that the Fe peaks are considerably suppressed, when compared with the uninhibited mild steel sample. This suppression of Fe lines is due to the inhibitory film formed on the mild steel surface. EDX analysis is in good aggrement with the results of polarization and impedance measurements, which suggest that the surface film inhibits the metal dissolution and retards the hydrogen evolution. The EDX analysis also validates the results obtained from gravimetric and electrochemical methods.

3.7. Atomic Force Microscopy. AFM is a powerful tool to investigate the surface morphology at nano- to microscale

dx.doi.org/10.1021/ie400815w | Ind. Eng. Chem. Res. XXXX, XXX, XXX−XXX

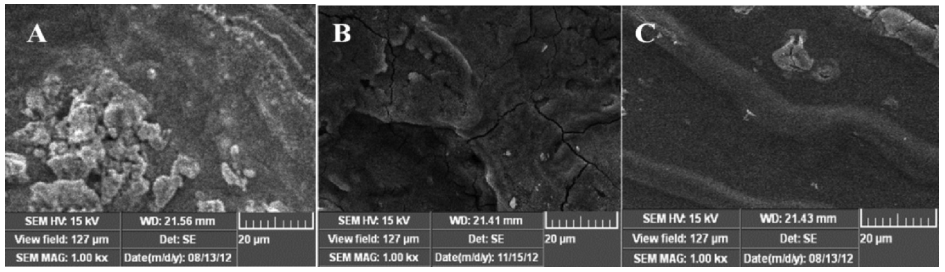

Figure 7. Scanning electron micrographs of a mild steel surface immersed for 3 h in (A) 1 N HCl, (B) 14×10^{-4} M furosemide, or (C) 14×10^{-4} M torsemide.

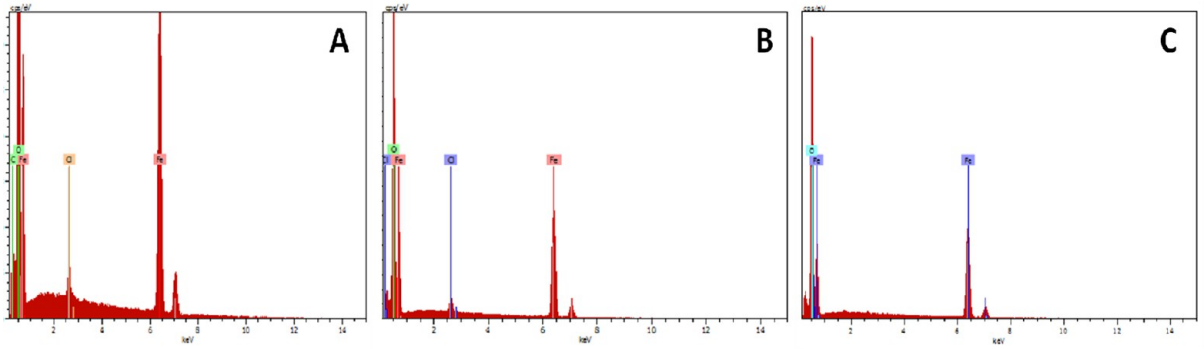

Figure 8. EDAX spectra of a mild steel surface immersed for 3 h in (A) 1 N HCl, (B) 14×10^{-4} M furosemide, and (C) 14×10^{-4} M torsemide.

levels. It has become a new method to investigate the nature of the protective layer formed on the mild steel surface.[55] AFM was used mainly for measuring the three-dimensional topography. Three-dimensional AFM images are given in Figure 9. Figure 9A is the image of a mild steel surface in 1 N HCl . Parts B and C of Figure 9 are images of a mild steel surface in the presence of an optimum concentration (14×10^{-4} M) of furosemide and torsemide, respectively. It is clear from the images that the surface of the specimen immersed in 1 N HCl is offering more roughness when compared to the specimens immersed in the solution containing furosemide and torsemide. The average roughness of the mild steel dipped in 1 N HCl was calculated to be 1360 nm. In the presence of an optimum concentration of furosemide and torsemide, the roughness was calculated to be 927 and 842 nm, respectively. The decrease in the roughness value is ascribed to the formation of the protective layer of furosemide and torsemide on the mild steel surface.

3.8. Mechanism of Inhibition. Generally the first stage in the corrosion inhibition mechanism is the adsorption of inhibitor molecules on the mild steel surface. The process of adsorption is influenced by the type of the aggressive electrolyte, the chemical structure of the inhibitor molecules, and the nature and charge of the metal. The charge on the metal surface is due to the electric field generated at the metal/electrolyte interface. It is reported that in acid solutions the mild steel surfaces are positively charged with respect to their potential zero charge (PZC).[56] The furosemide and torsemide may adsorb on the mild steel surface by

(i) electrostatic interaction of the inhibitor molecules with already adsorbed chloride ions (physisorption),
(ii) vacant d-orbitals of metal surface atoms and unshared electron pairs of heteroatoms (chemisorption), or
(iii) interaction of vacant the d-orbital of the inhibitor molecule with the d-electron of the metal surface (retrodonation).

In HCl medium the furosemide and torsemide molecules may adsorb through protonated heteroatoms (N, O, and S) and already adsorbed Cl^- ions on the mild steel surface. Initially the protonated forms of furosemide and torsemide in acid medium compete with H^+ ions for electrons on the mild steel surface. After the evolution of H_2 gas from 1 N HCl, the cationic form of inhibitors returns to its neutral form and heteroatoms with lone pair electrons promote chemical adsorption. The high electron density on the mild steel surface renders more negative charge to it. In order to relieve the surface from the high negative charge, the electron from the d-orbital of Fe may be transferred to the vacant π^*-orbital (antibonding) of the furosemide and torsemide molecules and in turn strengthen their adsorption on the mild steel surface.[57]

It is concluded from the experimental and theoretical results that the inhibition efficiency of torsemide is higher than that of furosemide. The weaker performance of furosemide is due to the presence of a chlorine atom; this chlorine atom has a negative inductive (−I) effect. Due to the −I effect, it increases the withdrawing nature of the ring and decreases the localization of the lone pair of electrons on the nitrogen atom. This reduces the formation of complex and decreases the inhibition efficiency. It should also be noted that the larger size and higher molecular weight of torsemide make it a better inhibitor of mild steel than furosemide.

The presence of exo-nitrogen, delocalized π-electrons, and imido groups is responsible for enhancement of electron density of the furosemide, which is responsible for effective adsorption of torsemide. In the case of furosemide, a −I effect of the chlorine atom may deplete the electron density, and hence, the adsorption of the latter is less facilitated on metal surfaces.

dx.doi.org/10.1021/ie400815w | Ind. Eng. Chem. Res. XXXX, XXX, XXX−XXX

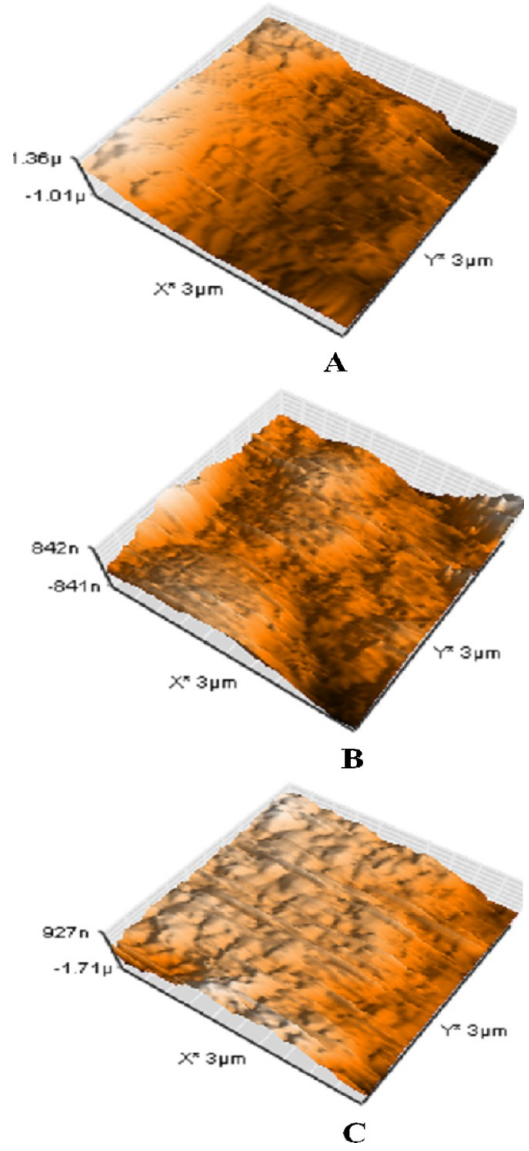

Figure 9. AFM images of a mild steel surface immersed for 3 h in (A) 1 N HCl, (B) 14×10^{-4} M furosemide, or (C) 14×10^{-4} M torsemide.

3.9. UV−Visible Spectroscopy. UV−visible spectroscopy gives the strongest evidence for the formation of metal−inhibitor complexes. UV−visible absorption spectra obtained for a 1 N HCl solution containing 14×10^{-4} M furosemide and torsemide before and after a 3 h immersion of mild steel at room temperature are shown in Figure 10.

The electronic absorption spectra of furosemide before immersion of mild steel showed two bands in the UV region at 230 and 270 nm, and that of torsemide also showed two bands at 210 and 285 nm. These bands may arise due to $\pi-\pi^*$ and $n-\pi^*$ transitions with a considerable charge transfer character. After 3 h of mild steel immersion, it is clear that there is an increase in the absorbance of the bands, which confirms the formation of Fe−inhibitor complexes in the solution. Obot et al.[58] reported that the shift in the value of absorbance indicates the complexation between two species in the solution. There is no significant change in the shape of the spectra before and after immersion of mild steel. The absorbance increase of torsemide is higher than that of furosemide, which proves that the interaction of torsemide with the iron surface is stronger than that of furosemide. This stronger interaction of torsemide leads to higher corrosion inhibition efficiency than that of furosemide. These experimental findings gave the strongest evidence for the formation of Fe−inhibitor complexes.

3.10. Infrared Spectroscopy. The comparison of the IR spectra of furosemide and torsemide powders with those of powders adsorbed on the mild steel are given Figure 11. In furosemide there is a shift from 3372 to 3437 cm^{-1} due to the N−H stretching. The bands corresponding to C−N at 1050 cm^{-1} dissappeared in spectral line a, which confirmed the interaction of the N−H group with the metal. The shift of the C═O and C−O stretching frequencies from 1658 to 1628 cm^{-1} and from 1417 to 1392 cm^{-1}, respectively, confirmed the adsorption of furosemide on the mild steel surface. In torsemide, the N−H stretching vibrations shift from 3350 to 3409 cm^{-1}. The peak at 1057 cm^{-1} due to C−N disappeared in spectrum a, which confirms the interaction of the C−N group with the metal. The shift of bands from 1644 to 1622 cm^{-1} and from 1417 to 1401 cm^{-1} due to the C═O and C—O stretching frequencies confirmed the interaction of torsemide with the mild steel surface. The shift in bands of the N−H stretching from lower wavenumber to higher wavenumber in both furosemide and torsemide may be due to the formation of an Fe−inhibitor complex on the surface. The bands at 479 and

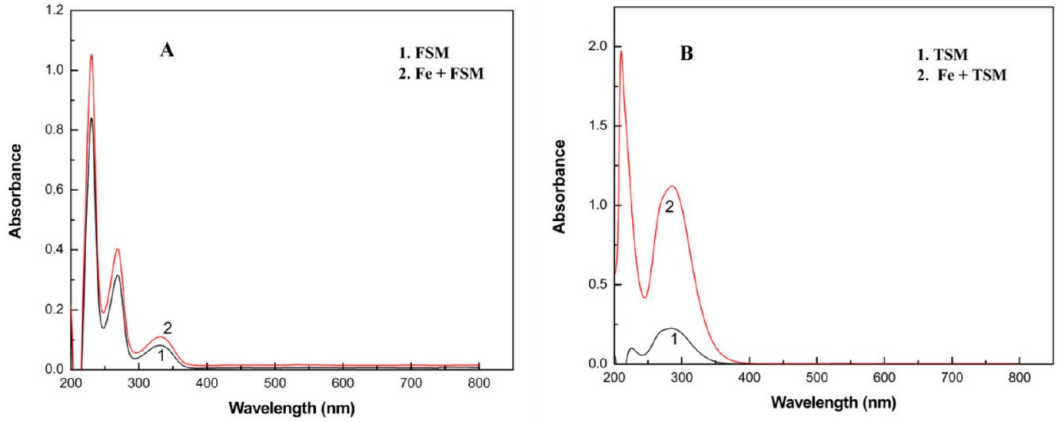

Figure 10. UV−visible spectra of a solution containing 14×10^{-4} M (A) furosemide or (B) torsemide before and after a 3 h immersion of mild steel in 1 N HCl.

dx.doi.org/10.1021/ie400815w | Ind. Eng. Chem. Res. XXXX, XXX, XXX−XXX

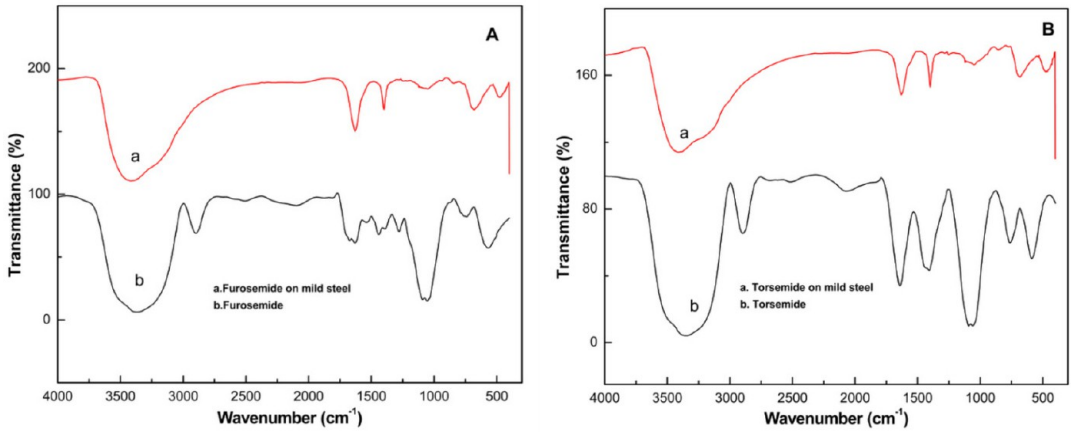

Figure 11. FT-IR spectra of (A) furosemide and (B) torsemide powders and the powders on the mild steel surface.

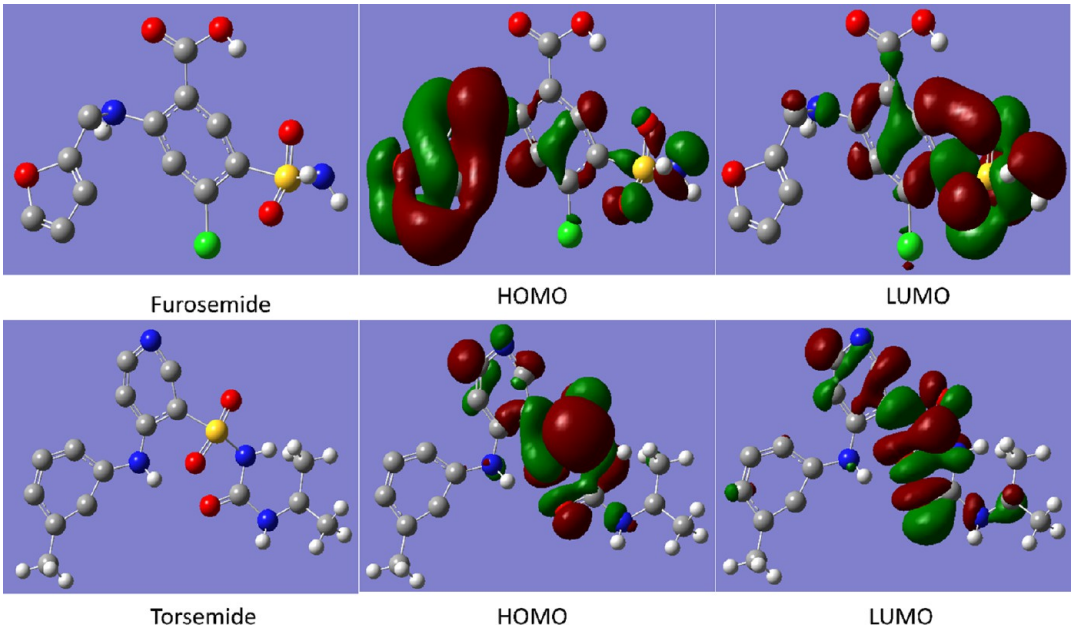

Figure 12. Optimized molecular structures, HOMOs, and LUMOs of the inhibitors.

471 cm^{-1} in the furosemide and torsemide adsorbed on the mild steel surfaces are due to the Fe−N stretching vibration.[59]

3.11. Theoretical Investigation. Quantum chemical methods have a strong impact toward the design and development of corrosion inhibitors. Density functional theory (DFT) has been used to precisely calculate information regarding molecular geometries and electron distributions. Due to its accuracy and smaller time requirement for the computational methods, it is widely used to analyze the inhibitor efficiencies and inhibitror surface interactions.[60] Hence, the DFT method was used to give some insight into the inhibitive mechanism of furosemide and torsemide molecules on the mild steel surface. Quantum chemical parameters such as E_{HOMO}, E_{LUMO}, the energy gap ΔE ($E_{LUMO} - E_{HOMO}$), and dipole moment (μ) were obtained for neutral furosemide and torsemide molecules to predict their activity toward a mild steel surface. These parameters were generated after geometric optimization with respect to all nuclear coordinates.

The ionization potential (I) and electron affinity (A) were calculated according to Koopmans theorem.[61] This theorem derives the relationship between the energies of the LUMO and HOMO, the ionization potential, and the electron affinity, respectively. A and I are related to E_{LUMO} and E_{HOMO} as follows:

$$A = -E_{LUMO}, \quad I = -E_{HOMO} \tag{14}$$

The absolute hardness (η) and absolute electronegativity (χ) of the inhibitor molecules are calculated from the following equations.

$$\chi = \frac{I + A}{2} \tag{15}$$

$$\eta = \frac{I - A}{2} \tag{16}$$

The softness (σ) can also be defined as

$$\sigma = \frac{1}{\eta} \tag{17}$$

Frontier molecular orbital theory is very useful in predicting the adsorption centers in furosemide and torsemide, which are

dx.doi.org/10.1021/ie400815w | Ind. Eng. Chem. Res. XXXX, XXX, XXX−XXX

Table 5. Quantum Chemical Parameters for Inhibitors Calculated with DFT Method

inhibitor	E_{HOMO} (eV)	E_{LUMO} (eV)	ΔE (eV)	μ (D)	η (eV)	σ (eV^{-1})	χ (eV)
furosemide	−0.2395	−0.1871	0.0524	4.3363	0.02622	38.138	0.2133
torsemide	−0.2787	−0.2605	0.0181	12.733	0.0090	110.55	0.2695

responsible for interaction with the metal surface.[62] Figure 12 shows the optimized structure and HOMO and LUMO densities of the furosemide and torsemide. It is seen from the figure that the HOMO and LUMO densities differ from each other for both the inhibitors. The HOMO and LUMO energy orbitals are mostly occupied on the heteroatoms present in both the inhibitors. The Mulliken charge analysis was used to estimate the adsorption centers of the inhibitors. It has been reported widely that the more negatively charged atoms have high ability to adsorb on the mild steel surface.

The adsorption of inhibitor molecules on the metal surface is due to the donor−acceptor interaction between inhibitor molecules and the metal surface. The electron donating ability of the molecule is associated with the E_{HOMO}. High values of E_{HOMO} indicate the tendency of inhibitor molecules to donate electrons to the acceptor molecules with empty molecular orbitals. The ability of a molecule to accept the electrons is related to E_{LUMO}. The lower value of E_{LUMO} indicates the easier acceptance of electrons from the metal surface and leads to higher inhibition efficiency.[63] The energy gap between the LUMO and HOMO energy levels, that is, ΔE of the molecule, is another important factor to determine the inhibition efficiency. The molecules with lower ΔE values give higher inhibition efficiencies because the excitation energy gap is more polarizable and is generally associated with chemical reactivity.[61] Dipole moment (μ) is an index that can be applied to discuss the molecule structure of the inhibitors. It was reported in the literature that the higher dipole moment increases the adsorption of inhibitors on the mild steel surface and increases the inhibition efficiency.[64,65] The reactivity parameters such as electronegativity (χ), global softness (σ), and global chemical hardness (η) are important properties to explain the molecular reactivity and stability. The large value of ΔE indicates the hard molecule, and the lower ΔE value corresponds to the soft molecule. Hence, the softer molecules are more reactive than harder molecules because of the lower ΔE values that facilitate an electron transfer process between inhibitor molecules and the mild steel surface.

Table 5 shows the calculated quantum chemical parameters. It can be observed from the table that the low ΔE value of torsemide indicates it as a softer molecule than furosemide. It also reveals that the lower ΔE and higher dipole moment (μ) of torsemide show its higher inhibiton efficiency when compared to furosemide, which is further evidenced from η and σ values . The higher inhibition efficiency of torsemide is further supported by the global reactivity parameters, that is, the lowest η value and higher σ value, as shown in the table. Both the inhibitors are donors of electrons, and the ability of torsemide to donate electrons is higher than that of furosemide. The calculated quantum chemical results were in good aggrement with the experimental values. The higher inhibition efficiency of torsemide is exhibited by the *N*-isopropyl formamide group attached to the sulfonamide group on the pyridine ring. It also has an excess number of heteroatoms when compared to furosemide, which plays a major role in the adsorption due to a lone pair of electrons. In the case of furosemide, the presence of a chlorine atom and fewer heteroatoms is the reason for its lower inhibition efficiency. It is concluded from the results that the quantum chemical calculations substantiated the experimental results.

4. CONCLUSIONS

(i) Furosemide and torsemide act as a very good inhibitor for mild steel in 1 N HCl solution, and the extent of inhibiton efficiency was dependent on the concentration of the inhibitors.

(ii) Tafel polarization curves proved that the compounds have been viewed as a mixed mode of inhibition. The impressive performance of the inhibitors has been confirmed from Nyquist plots. The mere adsorption of the inhibitors retarded C_{dl} and CPE at the expense of charge transfer resistance.

(iii) The adsorption model obeys the Langmuir adsorption isotherm. The ΔG°_{ads} and K_{ads} justified that furosemide and torsemide were strongly adsorbed on the mild steel surface.

(iv) The formation of Fe−furosemide and Fe−torsemide complexes was clearly indicated by UV−visible spectrophotometric studies. SEM, AFM, and FT-IR spectra results supported the formation of a film on the mild steel surface. Quantum chemical calculations substantiate the inhibition efficiencies obtained from experimental results.

(v) Among the two inhibitors, torsemide performance is superior to that of furosemide due to its high electron density, which favors its adsorption on the metal surface. The presence of a chlorine atom in the furosemide molecule deactivated the electron density and justified its inferior performance in the 1 N HCl medium.

■ ASSOCIATED CONTENT

Supporting Information

Results of weight loss method, Arrhenius plots, Gibbs free energy parameters, and thermodynamic parameters for mild steel in 1 N HCl without and with different concentrations of furosemide and torsemide at various temperatures. This material is available free of charge via the Internet at http://pubs.acs.org.

■ AUTHOR INFORMATION

Corresponding Author

*E-mail: skarthikeyanphd@yahoo.co.in. Telephone: +91-416-2205708, +91-9585587561.

Notes

The authors declare no competing financial interest.

■ ACKNOWLEDGMENTS

The authors would like to express their sincere thanks to the Chancellor,Vice Presidents, and all core group members of VIT University, Vellore, India, for their constant encouragement and support extended to carry out this research.

REFERENCES

(1) Ashassi-Sorkhabi, H.; Seifzadeh, D.; Hosseini, M. G. EN, EIS and polarization studies to evaluate the inhibition effect of 3H-phenothiazin3-one, 7-dimethylamin on mild steel corrosion in 1M HCl solution. *Corros. Sci.* **2008**, *50*, 3363.

(2) Ameer, M. A.; Khamis, E.; Al-Senani, G. Adsorption studies of the effect of thiosemicarbazides on the corrosion of steel in phosphoric acid. *Adsorpt. Sci. Technol.* **2000**, *18*, 177.

(3) Morad, M. S.; Kamal El-Dean, A. M. 2,2′-Dithiobis(3-cyano-4,6-dimethylpyridine): A new class of acid corrosion inhibitors for mild steel. *Corros. Sci.* **2006**, *48*, 3398.

(4) Popova, A.; Sokolova, E.; Raicheva, S.; Christov, M. AC and DC study of the temperature effect on mild steel corrosion in acid media in the presence of benzimidazole derivatives. *Corros. Sci.* **2003**, *45*, 33.

(5) Moretti, G.; Guidi, F.; Grion, G. Tryptamine as a green iron corrosion inhibitor in 0.5 M deaerated sulphuric acid. *Corros. Sci.* **2004**, *46*, 387.

(6) Singh, A. K. Inhibition of Mild Steel Corrosion in Hydrochloric Acid Solution by 3-(4-((Z)-Indolin-3-ylideneamino)phenylimino)-indolin-2-one. *Ind. Eng. Chem. Res.* **2012**, *51*, 3215.

(7) Chidiebere, M. A.; Ogukwe, C. E.; Oguzie, K. L.; Eneh, C. N.; Oguzie, E. E. Corrosion Inhibition and Adsorption Behavior of Punica granatum Extract on Mild Steel in Acidic Environments: Experimental and Theoretical Studies. *Ind. Eng. Chem. Res.* **2012**, *51*, 668.

(8) Yadav, D. K.; Quraishi, M. A. Electrochemical investigation of Substituted Pyranopyrazoles Adsorption on Mild Steel in Acid Solution. *Ind. Eng. Chem. Res.* **2012**, *51*, 8194.

(9) Mayakrishnan, G.; Nagamani, S.; Devarayan, K.; Ick Soo, K.; Ramasamy, K. Chemical and Physical Interactions of 1-Benzoyl-3,3-Disubstituted Thiourea Derivatives on Mild Steel Surface: Corrosion Inhibition in Acidic Media. *Ind. Eng. Chem. Res.* **2012**, *51*, 7910.

(10) Bentiss, F.; Bouanis, M.; Mernari, B.; Traisnel, M.; Vezin, H.; Lagrenee, M. Understanding the adsorption of 4H- 1,2,4-triazole derivatives on mild steel surface in molar hydrochloric acid. *Appl. Surf. Sci.* **2007**, *253*, 3696.

(11) Abd El-Maksoud, S. A.; Hassan, H. H. Electrochemical studies on the effect of (2E)-3-amino-2-phenylazo-but-2-enenitrile and its derivative on the behaviour of copper in nitric acid. *Mater. Corros.* **2007**, *58*, 369.

(12) Fu, J. J.; Zang, H. S.; Wang, Y.; Li, S. N.; Chen, T.; Liu, X. D. Experimental and Theoretical Study on the Inhibition Performances of Quinoxaline and Its Derivatives for the Corrosion of Mild Steel in Hydrochloric Acid. *Ind. Eng. Chem. Res.* **2012**, *51*, 6377.

(13) Trabanelli, G. In *Corrosion Mechanisms*; Mansfeld, F., Ed.;Marcel Dekker: New York, 1987.

(14) Rozenfeld, I. L. *Corrosion Inhibitors*; McGraw-Hill Inc.: 1981; p 97.

(15) Thomas, J. G. N. *Proceedings of the 5th European Symposium on Corrosion Inhibitors*; Università degli Studi di Ferrara, September 15–19, 1980; p 453.

(16) Abdallah, M. Rhodanine azosulpha drugs as corrosion inhibitors for corrosion of 304 stainless steel in hydrochloric acid solution. *Corros. Sci.* **2002**, *44*, 717.

(17) Abdallah, M. Antibacterial drugs as corrosion inhibitors for corrosion of aluminium in hydrochloric solution. *Corros. Sci.* **2004**, *46*, 1981.

(18) Prabhu, R. A.; Shanbhag, A. V.; Venkatesha, T. V. Influence of tramadol [2-[(dimethylamino)methyl]-1-(3-methoxyphenyl)-cyclohexanolhydrate] on corrosion inhibition of mild steel in acidic media. *J. Appl. Electrochem.* **2007**, *37*, 491.

(19) El-Naggar, M. Corrosion inhibition of mild steel in acidic medium by some sulfa drugs compounds. *Corros. Sci.* **2007**, *49*, 2226.

(20) Morad, M. S. Inhibition of iron, corrosion in acid solutions by Cefatrexyl: Behaviour near and at the corrosion potential. *Corros. Sci.* **2008**, *50*, 436.

(21) Shukla, S. K.; Singh, A. K.; Ahamad, I.; Quraishi, M. A. Streptomycin: A commercially available drug as corrosion inhibitor for mild steel in hydrochloric acid solution. *Mater. Lett.* **2009**, *63*, 819.

(22) Shukla, S. K.; Quraishi, M. A. Cefotaxime sodium: A new and efficient corrosion inhibitor for mild steel in hydrochloric acid solution. *Corros. Sci.* **2009**, *51*, 1007.

(23) Obot, I. B.; Obi-Egbedi, N. O.; Umoren, S. A. Antifungal drugs as corrosion inhibitors for aluminium in 0.1 M HCl. *Corros. Sci.* **2009**, *51*, **1868**.

(24) Ahamad, I.; Prasad, R.; Quraishi, M. A. Inhibition of mild steel corrosion in acid solution by Pheniramine drug. Experimental and theoretical study. *Corros. Sci.* **2010**, *52*, 3033.

(25) Ahamad, I.; Quraishi, M. A. Mebendazole: New and efficient corrosion inhibitor for mild steel in acid medium. *Corros. Sci.* **2010**, *52*, 651.

(26) Singh, A. K.; Quraishi, M. A. Effect of Cefazolin on the corrosion of mild steel in HCl solution. *Corros. Sci.* **2010**, *52*, 152.

(27) ASTM G-31-72, Standard practice for laboratory immersion corrosion testing of metals; ASTM: Philadelphia, PA, 1990.

(28) Singh, A.; Ahamad, I.; Singh, V. K.; Quraishi, M. A. The inhibition effect of environmentally benign Karaanj (Pongamia pinnata) seed extracts on corrosion of mild steel in hydrochloric acid solution. *J. Solid State Electrochem.* **2011**, *11*, 1087.

(29) Khaled, K. F.; Amin, M. A. Corrosion monitoring of mild steel in sulphuric acid solutions in presence of some thiazole derivatives – Molecular dynamics. *Chem. Electrochem. Stud.* **2009**, *51*, 1964.

(30) Hassan, H. H.; Abdelghani, E.; Amin, M. A. Inhibition of mild steel corrosion in hydrochloric acid solution by triazole derivatives Part I. Polarization and EIS studies. *Electrochim. Acta* **2007**, *52*, 6359.

(31) Negam, N. A.; Kandile, N. G.; Aiad, I. A.; Mohammad, M. A. New eco-friendly cationic surfactants: Synthesis, characterization and applicability as corrosion inhibitors for carbon steel in 1N HCl. *Colloids Surf., A* **2011**, *391*, 224.

(32) Quartarone, G.; Bonaldo, L.; Tortato, C. Inhibitive action of indole-5-carboxylic acid towards corrosion of mild steel in deaerated 0.5M sulfuric acid solution. *Appl. Surf. Sci.* **2006**, *252*, 8251.

(33) Tamil Selvi, S.; Raman, V.; Rajendran, N. Corrosion inhibition of mild steel by benzotriazole derivatives in acidic medium. *J. Appl. Electrochem.* **2003**, *33*, 1175.

(34) Ferreira, E. S.; Giancomelli, C.; Giancomelli, F. C.; Spinelli, A. Evaluation of the inhibitor effect of l-ascorbic acid on the corrosion of mild steel. *Mater. Chem. Phys.* **2004**, *83*, 129.

(35) Riggs, O. L. Jr. *Corrosion Inhibitors*, 2nd ed.; Nathan, C. C., Ed.; NACE: Houston, TX, USA, 1973; p 109.

(36) Oguzie, E. E.; Lia, Y.; Wang, F. H. Effect of 2-amino-3-mercaptopropanoic acid (cysteine) on the corrosion behavior of low carbon steel in sulphuric acid. *Electrochim. Acta* **2007**, *53*, 909.

(37) Lenderink, H. J. W.; Linden, M. V. D.; De Wit, J. H. W. Corrosion of aluminium in acidic and neutral solutions. *Electrochim. Acta* **1993**, *38*, 1989.

(38) Bentiss, F.; Mehdi, B.; Mernari, B.; Traisnal, M.; Vezin, H. Electrochemical and quantum chemical studies of 3,5-di(n-tolyl)-4-amino-1,2,4-triazole adsorption on mild steel in acidic media. *Corrosion* **2002**, *58*, 399.

(39) Martinez, S.; Stern, I. Thermodynamic characterization of metal dissolution and inhibitor adsorption process in the low carbon steel/mimosa tannin/sulfuric acid system. *Appl. Surf. Sci.* **2002**, *199*, 83.

(40) El Sherbini, E. F. Effect of some ethoxylated fatty acids on the corrosion behaviour of mild steel in sulphuric acid solution. *Mater. Chem. Phys.* **1999**, *60*, 286.

(41) Szauer, T.; Brand, A. Mechanism of inhibition of electrode reactions at high surface coverages—II. *Electrochim. Acta* **1981**, *26*, 1219.

(42) Morad, M. S.; Kamal El-Dean, A. M. 2,2′-Dithiobis(3-cyano-4,6-dimethylpyridine): A new class of corrosion inhibitors for mild steel. *Corros. Sci.* **2006**, *48*, 3398.

(43) Ashassi-Sorkhabi, H.; Shaabani, B.; Seifzadeh, D. Corrosion inhibition of mild steel by some Schiff base compounds in hydrochloric acid. *Appl. Surf. Sci.* **2005**, *239*, 154.

(44) Guan, N.; Xueming, M. L.; Fei, L. Synergistic inhibition between o-phenanthroline and chloride ion on cold rolled steel corrosion in phosphoric acid. *Mater. Chem. Phys.* **2004**, *86*, 59.

(45) Khamis, E.; Hosney, A.; El-Khodary, S. *Afindad* **1995**, *52*, 95–106.
(46) Vracar, L. J.; Drazic, D. M. Adsorption and corrosion inhibitive properties of some organic molecules on iron electrode in sulfuric acid. *Corros. Sci.* **2002**, *44*, 1669.
(47) Tang, L.; Mu, G.; Liu, G. The effect of neutral red on the corrosion inhibition of cold rolled steel in 1.0 M hydrochloric acid. *Corros. Sci.* **2003**, *45*, 2251.
(48) Keles, H.; Keles, M.; Dehri, I.; Serindag, O. Adsorption and inhibitive properties of aminobiphenyl and its Schiff base on mild steel corrosion in 0.5M HCl medium. *Colloids Surf., A* **2008**, *320*, 138.
(49) Kumar, M. S.; Kumar, S. L. A.; Sreekanth, A. Anticorrosion potential of 4-amino 3-methyl-1,2,4-triazole-5-thione derivatives (SAMTT and DBAMTT) on Mild steel in Hydrochloric acid solution. *Ind. Eng. Chem. Res.* **2012**, *51*, 5408.
(50) Singh, A. K.; Quaraishi, M. A. Inhibitive effect of diethylcarbamazine on the corrosion of mild steel in hydrochloric acid. *Corros. Sci.* **2010**, *52*, 1529.
(51) Li, X.; Deng, S.; Fu, H.; Li, T. Adsorption and inhibition effect of 6-benzylaminopurine on cold rolled steel in 1.0 M HCl. *Electrochim. Acta* **2009**, *54*, 4089.
(52) Li, X. H.; Deng, S. D.; Fu, H.; Mu, G. N. Synergistic inhibition effect of rare earth cerium(IV) ion and anionic surfactant on the corrosion of cold rolled steel in H_2SO_4 solution. *Corros. Sci.* **2008**, *50*, 2635.
(53) Zhao, T. P.; Mu, G. N. The adsorption and corrosion inhibition of anion surfactants on aluminium surface in hydrochloric acid. *Corros. Sci.* **1999**, *4*, 1937.
(54) Durnie, W.; De Marco, R.; Kinsella, B.; Jefferson, A. Development of a Structure-Activity Relationship for Oil Field Corrosion Inhibitors. *J. Electrochem. Soc.* **1999**, *146* (5), 1751.
(55) Quaraishi, M. A.; Singh, A.; Singh, V.; Yadav, D.; Singh, A. K. Green approach to corrosion inhibition of mild steel in hydrochloric acid and sulfuric acid solutions by the extract of Murraya koenigii leaves. *Mater. Chem. Phys.* **2010**, *122*, 114.
(56) Deng, S.; Li, X.; Fu, H. Acid violet 6B as a novel corrosion inhibitor for cold rolled steel in hydrochloric acid solution. *Corros. Sci.* **2011**, *53*, 760.
(57) Xometl, O. O.; Likhanova, N. V.; Anguilar, M. A. D.; Arce, E.; Dorantes, H.; Lozada, P. A. Synthesis and corrosion inhibition of α-amino acids alkylamides for mild steel in acid environment. *Mater. Chem. Phys.* **2008**, *110*, 344.
(58) Obot, I. B.; Obi-Egbedi, N. O.; Eseola, A. O. Anticorrosion Potential of 2-Mesityl-1H-imidazo[4,5-f][1,10]-phenanthroline on Mild Steel in Sulfuric Acid Solution: Experimental and Theoretical Study. *Ind. Eng. Chem. Res.* **2011**, *50*, 2098.
(59) Li., X.; Deng, S.; Fu, H.; Mu, G. Inhibition effect of 6-benzylaminopurine on the corrosion of cold rolled steel in H2SO4 solution. *Corros. Sci.* **2009**, *51*, 620.
(60) Obi-Egbedi, N. O.; Obot, I. B.; El-Khaiary, M. I. Quantum chemical investigation and statistical analysis of the relationship between corrosion inhibition efficiency and molecular structure of xanthenes and its derivatives on mild steel in sulphuric acid. *J. Mol. Struct.* **2011**, *1–3*, 86.
(61) Awad, M. K.; Mustafa, M. R.; Elnga, M. M. A. Computational simulation of the molecular structure of some triazoles as inhibitors for the corrosion of metal surface. *THEOCHEM* **2010**, *959*, 1.
(62) Masoud, M. S.; Awad, M. K.; Shaker, M. A.; El-Tahawy, M. M. T. The role of structural chemistry in the inhibitive performance of some aminopyrimidines on the corrosion of steel. *Corros. Sci.* **2010**, *52*, 2387.
(63) Hasanov, R.; Bilge, S.; Bilgic, S.; Gece, G.; Kilic, Z. Experimental and theoretical calculations on corrosion inhibition of steel in 1M H2SO4 by crown type polyesters. *Corros. Sci.* **2010**, *52*, 984.
(64) Li, X.; Deng, S.; Fu, H. Adsorption and inhibition effect of vanillin on cold rolled steel in 3.0M H3PO4. *Prog. Org. Coat.* **2010**, *67*, 420.
(65) Khalil, N. Quantum chemical approach of corrosion inhibition. *Electrochim. Acta* **2003**, *48*, 2635.

dx.doi.org/10.1021/ie400815w | *Ind. Eng. Chem. Res.* XXXX, XXX, XXX–XXX